

**Supporting Information for  
“Detecting Urban Emissions Changes and Events with a Near-Real-Time-  
Capable Inversion System”**

**John Ware<sup>1,2</sup>, Eric A. Kort<sup>2</sup>, Riley Duren<sup>3</sup>, Kimberly L Mueller<sup>2,4</sup>, Kristal Verhulst<sup>3</sup>, Vineet  
Yadav<sup>3</sup>**

<sup>1</sup>Department of Physics, University of Michigan, Ann Arbor, Michigan, USA

<sup>2</sup>Department of Climate and Space Sciences and Engineering, University of Michigan, Ann Arbor, Michigan, USA

<sup>3</sup>NASA Jet Propulsion Laboratory, California Institute of Technology, Pasadena, California, USA

<sup>4</sup>National Institute of Standards and Technology (NIST); Gaithersburg, MD, United States of America

**Contents**

1. Figures S1 to S3
2. Tables S1 to S2

---

Corresponding author: John Ware, [johnware@umich.edu](mailto:johnware@umich.edu)

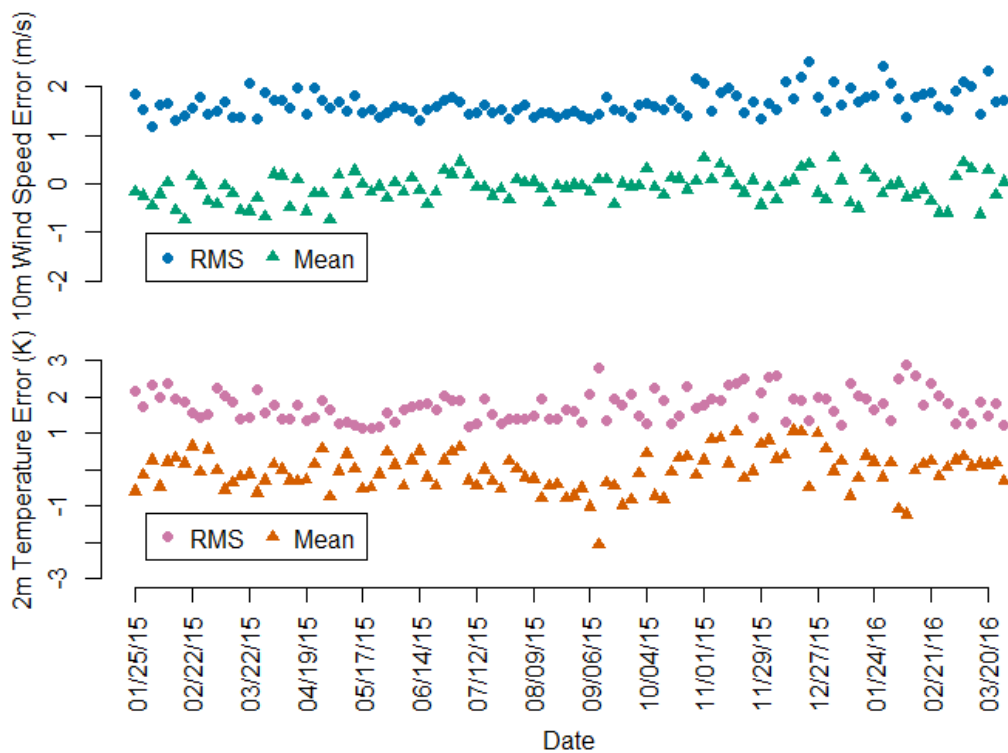


**Figure 1.** Time series of bias and RMS errors in WRF-simulated 2 m temperature (bottom) and 10 m wind speed (top) as compared to surface station observations.

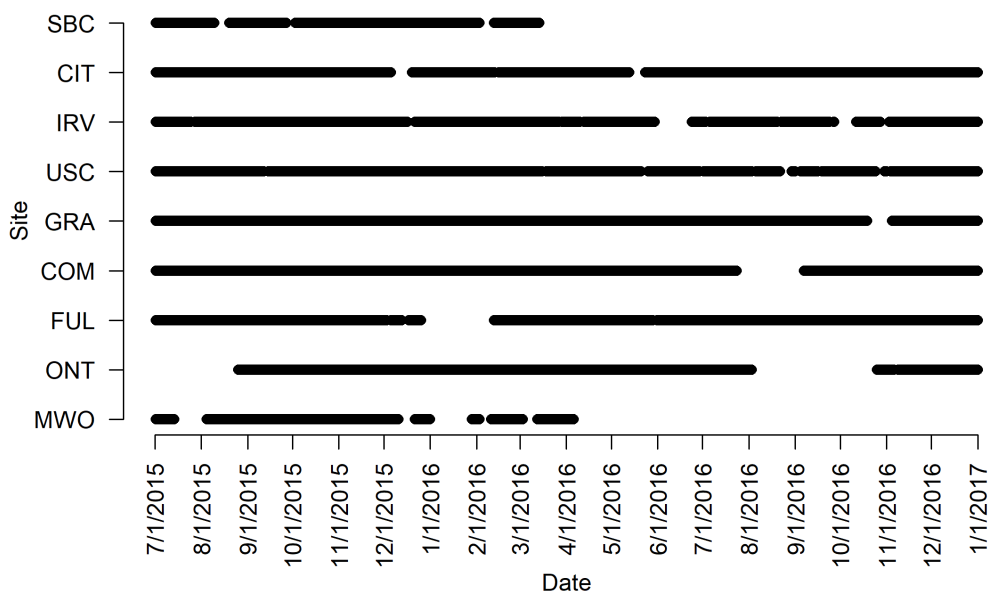


**Figure 2.** Availability of mole fraction data for each of the nine sites within the SOCAB domain used in this study.

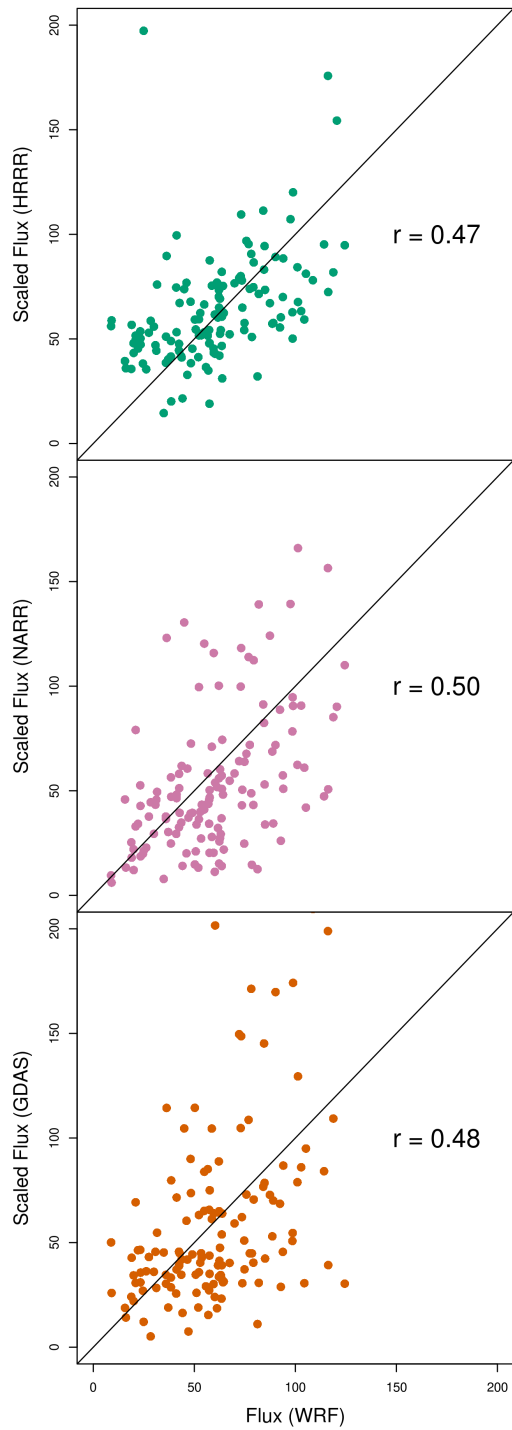


**Figure 3.** Scatter plots of four-day methane flux estimates from the WRF-driven inversion as compared to the corresponding fluxes from the HRRR-, NARR-, and GDAS-driven inversions after applying calibration. The correlation coefficient between the calibrated fluxes and the WRF-derived fluxes is inset in each case.

Option	Description
Land Surface	Noah land-surface model with Monin-Obukov (Janic) surface layer
Urban Canopy	None
PBL Package	MYNN 2.5-level scheme
LW Radiation	RRTMG
SW Radiation	RRTMG
Microphysics	WSM 5-class scheme
Convection	Grell-3d (in outer domains)
Nesting	One-way
Nudging	None
Advection	5th-order horizontal, 3rd-order vertical, monotonic advection for moisture and scalars
Diffusion	2nd-order horizontal diffusion using Smagorinsky first-order closure

**Table 1.** Summary of WRF options used.

Period	HRRR		NARR		GDAS	
	Predicted	Actual	Predicted	Actual	Predicted	Actual
1	106%*	70%	76%*	121%	158%*	194%
2	94%*	52%	64%*	91%	139%	154%
3	64%	60%	52%*	151%	122%*	176%
4	65%	55%	54%	52%	97%*	68%
5	66%*	43%	45%*	102%	71%*	113%
6	65%*	32%	45%*	68%	58%*	92%
7	71%	54%	42%	60%	67%	86%
8	83%*	46%	38%*	81%	62%*	100%
9	88%*	43%	37%*	82%	55%	73%
10	64%	56%	36%*	120%	59%*	174%
11	85%*	65%	54%*	110%	97%*	140%
12	76%	70%	60%*	81%	92%*	154%
13	93%*	62%	56%*	98%	104%*	135%
14	76%	80%	54%*	109%	116%*	184%
15	88%	81%	73%	78%	145%*	196%
16	81%	76%	54%*	116%	132%*	168%
17	110%*	57%	68%*	214%	113%	115%
18	88%*	51%	70%*	101%	89%	72%
19	86%*	56%	64%*	107%	70%*	140%

**Table 2.** Actual: total mean sensitivity of observations in each of nineteen 28-day periods according to STILT footprints driven by HRRR, NARR, and GDAS, relative to sensitivity according to footprints driven by WRF. Predicted: Sensitivity relative to WRF, over the same time period, predicted as in Equation 3 on the basis of residence time, near-surface fraction, and mixing height. Predicted values marked with asterisks differ from actual values by more than 20 percentage points.